Redox Biology 14 (2018) 535–548

Contents lists available at ScienceDirect

Redox Biology

journal homepage: www.elsevier.com/locate/redox

Research Paper

α-Lipoic acid improves abnormal behavior by mitigation of oxidative stress, inflammation, ferroptosis, and tauopathy in P301S Tau transgenic mice

Yan-Hui Zhang[a], Da-Wei Wang[b], Shuang-Feng Xu[a], Shuai Zhang[a], Yong-Gang Fan[a], Ying-Ying Yang[a], Shi-Qi Guo[a], Shan Wang[a], Tian Guo[a], Zhan-You Wang[a,*], Chuang Guo[a,*]

[a] College of Life and Health Sciences, Northeastern University, No.195, Chuangxin Road, Hunnan District, Shenyang 110169, China
[b] China Medical University-The Queen's University of Belfast Joint College, No.77 Puhe Road, Shenyang North New Area, Shenyang 110122, China

ARTICLE INFO

Keywords:
Tau
α-Lipoic acid
Oxidative stress
Ferroptosis
Alzheimer's disease

ABSTRACT

Alzheimer's disease (AD) is the most common neurodegenerative disease and is characterized by neurofibrillary tangles (NFTs) composed of Tau protein. α-Lipoic acid (LA) has been found to stabilize the cognitive function of AD patients, and animal study findings have confirmed its anti-amyloidogenic properties. However, the underlying mechanisms remain unclear, especially with respect to the ability of LA to control Tau pathology and neuronal damage. Here, we found that LA supplementation effectively inhibited the hyperphosphorylation of Tau at several AD-related sites, accompanied by reduced cognitive decline in P301S Tau transgenic mice. Furthermore, we found that LA not only inhibited the activity of calpain1, which has been associated with tauopathy development and neurodegeneration via modulating the activity of several kinases, but also significantly decreased the calcium content of brain tissue in LA-treated mice. Next, we screened for various modes of neural cell death in the brain tissue of LA-treated mice. We found that caspase-dependent apoptosis was potently inhibited, whereas autophagy did not show significant changes after LA supplementation. Interestingly, Tau-induced iron overload, lipid peroxidation, and inflammation, which are involved in ferroptosis, were significantly blocked by LA administration. These results provide compelling evidence that LA plays a role in inhibiting Tau hyperphosphorylation and neuronal loss, including ferroptosis, through several pathways, suggesting that LA may be a potential therapy for tauopathies.

1. Introduction

Tau is a microtubule-associated protein, and its hyperphosphorylation and abnormal aggregation together with synaptic and neuronal degeneration have been regarded as the principal neuropathological hallmark of neurodegenerative tauopathies including Alzheimer's disease (AD) [1,2]. Reducing the overall levels of Tau or preventing its hyperphosphorylation and accumulation have been shown to have therapeutic benefits, although it remains unclear how Tau contributes to the dysfunction and degeneration involved in AD [3,4]. Numerous studies have demonstrated that Tau is relevant to oxidative stress [5,6], and several mechanisms related to oxidative stress and free-radical reactions are involved in the formation of neurofibrillary tangles (NFTs) [7]. In the search for the causes of oxidative stress, progressive iron accumulation in the normal aging brain and an aberrantly elevated iron level in the AD brain have been identified [8,9]. Through Fenton's reaction, iron overload can generate excessive free radicals that attack DNA, proteins, and lipid membranes, thereby damaging cellular function and causing neuronal death. In particular, iron can bind to Tau protein [10,11] and trigger its hyperphosphorylation [12], eventually leading to the formation of NFTs [13]. Thus, either reducing the redox activity of the iron-Tau interaction or rescuing neurons directly could be potential therapies for treating tauopathy.

α-Lipoic acid (LA), a naturally occurring enzyme cofactor with antioxidant and iron chelator [14] properties, has been used as a therapeutic agent for many chronic diseases such as diabetes mellitus (DM) and the associated peripheral neuropathy. Importantly, LA was also found to provide neuroprotection against AD, as it can easily penetrate the blood-brain barrier (BBB). The therapeutic effect of LA for AD was found by chance in clinical trials that demonstrated that LA supplementation could moderate the cognitive functions of patients with AD and related dementias [15,16]. In previous animal studies, LA supplementation improved cognition and memory in aged SAMP8 mice and aged rats [17,18], reduced hippocampal-dependent memory deficits in the Tg2576 model of AD without affecting β-amyloid (Aβ) levels or

* Corresponding authors.
E-mail addresses: wangzy@mail.neu.edu.cn (Z.-Y. Wang), guoc@mail.neu.edu.cn (C. Guo).

http://dx.doi.org/10.1016/j.redox.2017.11.001
Received 13 September 2017; Received in revised form 27 October 2017; Accepted 1 November 2017
2213-2317/ © 2017 The Authors. Published by Elsevier B.V. This is an open access article under the CC BY-NC-ND license (http://creativecommons.org/licenses/BY-NC-ND/4.0/).

plaque deposition [19], and restored glucose metabolism and synaptic plasticity in the triple transgenic mouse model of AD [20,21]. In vitro studies relevant to AD mechanisms have revealed that LA can inhibit the formation of Aβ fibrils (fAβ) and the stabilization of preformed fAβ, as well as protect cultured hippocampal neurons against neurotoxicity induced by Aβ and iron/hydrogen peroxide [22,23]. Based on the above facts, it has been proposed that these actions are mediated through potent antioxidant [24], anti-inflammatory [25], and anti-amyloidogenic properties [22,23]. Moreover, LA itself is not only an efficient free radical scavenger, but the disulfide bond and five-membered cyclic structure of LA lead to powerful antioxidant capacity and good iron-chelation activity [14,26]. These multifaceted effects suggest that LA is a promising therapeutic agent for AD, but the exact cellular and molecular mechanisms remain unknown, especially with respect to the ability of LA to control Tau pathology and neuronal damage. In this context, we previously showed that the hyperphosphorylation status of Tau can be reversed by iron chelation in an AD mouse model [27].

In fact, LA plays many different roles in the pathogenic pathways of dementia, acting as a neuroprotective agent. LA might attenuate free radical damage and reduce inflammatory activities and, hence, might have a positive effect on neuronal ferroptosis, which is a recently discovered form of cell death dependent on iron and ROS [28], because ferroptosis can also be prevented by ferrostain-1, lipophilic antioxidants and iron chelators, such as deferoxamine [29,30]. In the present study, P301S mice encoding the human P301S mutation were injected with LA for 10 weeks to study whether LA could effectively alleviate the state of AD-related tauopathy and whether the inhibition of ferroptosis is a potential mechanism of restoring impaired cognition.

2. Materials and methods

2.1. Animals and pharmacological treatments

The P301S transgenic mice [B6C3-Tg (Prnp-MAPT*P301S) PS19 Vle/J], originally obtained from the Jackson laboratory (Bar Harbor, ME, USA), were used as a model of tauopathy. The mice were housed in standard environmental conditions at an ambient temperature of 20–26 °C and humidity of 40–70%. They were raised with 5 mice per cage, free food and water, and the natural circadian rhythm of light. The female mice at the age of 5 months were randomly allocated to three treatment groups (7 mice/group) corresponding to vehicle control, 3 mg/kg LA (T5625, Sigma, St. Louis, MO; the dosage was calculated everyday based on weight), and 10 mg/kg LA. LA was administered by intraperitoneal injection once per day (no injection was administered one day every three days), and vehicle control mice received physiological saline. The body mass and health conditions of the mice were monitored and recorded daily. After the cumulative injection time reached 10 weeks, the mice were evaluated by a series of behavioral tests. All treatments were performed in accordance with the National Institutes of Health guidelines, and experimental procedures were approved by the Laboratory Animal Ethical Committee of Northeastern University.

2.2. Open field test

The open field test (OFT) is a typical method used to study spontaneous motor activity and exploratory behaviors. All mice in each group were allowed to adapt to the new experimental environment for 30 min before the test was begun. The OFT was carried out in a quiet environment. The mouse was placed in the center of the arena, and the digital camera recorded the mouse for 5 min of continuous acquisition. The amount of time spent in the center of the arena and the total distance traveled were collected by SMART 3.0 software. To prevent interference between trials, the inner wall and bottom of the arena were cleaned during the inter-trial interval.

2.3. Morris water maze

The Morris water maze (MWM) was employed to measure spatial learning and memory by requiring navigation. A circular pool (diameter 90 cm) was filled with water before the test was begun, and the water was maintained at a constant temperature of 24 °C. The area of the pool was divided into four imaginary quadrants for analysis of the test and probe trials. Mice were first trained to find a visible platform located 1 cm above the water (nonspatial learning, days 1–3) and then trained to find a hidden platform submerged 1 cm beneath the surface of the water (spatial learning, days 4–7). During visible platform training, mice remained on the platform for 15 s before returning to the home cage, and this process was repeated until all the mice were able to find the platform position. Mice that had difficulty swimming and non-performers were removed from the trial. Mice were placed in the pool facing the wall and carefully released. For each trial, the computer tracking program SMART 3.0 began recording immediately when the mouse entered the water. Each trial was limited to 1 min. When the mouse climbed onto the platform or the time ran out, the computer program automatically ended the recording. During the visible and hidden platform training sessions, the platform remained in the same quadrant at the same starting location. Relevant data such as latency, path length and time in the target quadrant were acquired by the computer program in this process. Four trials of training were conducted per day with an inter-trial interval of 30 min.

A probe trial was performed on day 8. The platform was removed, and the mice were allowed to swim freely in the pool for 1 min. For the probe trial, the time spent in the quadrant of the former platform position and the number of crossings of the exact place where the platform had been located were acquired by the SMART 3.0 computer program.

2.4. Novel object recognition test

The novel object recognition test (NOR) is based on the natural tendency of mice to explore a novel or displaced object more than a familiar object. The test was carried out in three phases. In the first stage, animals were allowed to move freely in a 40 × 40 × 40 cm^3 gray resin box for adaptation, and the adaptation trial was conducted over 3 consecutive days for 10 min/d. On the fourth day, two identical objects were presented in the box, as shown in Fig. 7I, the exploration time was recorded in 10 min. Animals exhibiting any investigative behavior (head orientation or sniffing occurring) or entering the area within 1 cm around the object was considered exploration behavior. In the testing trial performed on the fifth day, one of the familiar objects was replaced by a novel object with a different shape, color and material, and the exploration times of the familiar and novel objects in 10 min were acquired by the SMART 3.0 computer system. The acquired data were then analyzed to assess the learning and memory ability of the mice.

2.5. Western blots

All animals were sacrificed at the end of the behavioral tests. The brain was immediately removed and cut in half on an ice box. Half was stored in 4% paraformaldehyde for immunohistochemistry and immunofluorescence, and the other half was stored in −80 °C refrigerator prior to use for Western blots. Well-mixed lysis buffer (phosphatase inhibitor cocktail, protease inhibitor cocktail, sodium fluoride and phenylmethanesulfonyl fluoride added to radioimmunoprecipitation assay [RIPA] lysis buffer at a 1:100 ratio) was added to the samples. Then, the samples were treated with ultrasonic crash, and the homogenate was centrifuged at 12,000 rpm for 25 min at 4 °C. The supernatants containing 30 μg protein were loaded into 10% or 12% SDS-PAGE to separate proteins and then transferred onto polyvinylidene difluoride (PVDF) membranes (Millipore, IPVH00010). The membranes were incubated with only one primary antibody overnight in a 4 °C

refrigerator after blocking by 5% skim milk. The primary antibodies used in the study were as follows: mouse-anti-apoptosis inducing factor (AIF, 1:1000, Santa Cruz), mouse-anti-Bcl2 (1:1000, Santa Cruz), rabbit-anti-Bax (1:1000, Santa Cruz), mouse-anti-Beclin1 (1:1000, ImmunoWay), rabbit-anti-calpain1 (1:2000, Abcam), rabbit-anti-p-cyclin dependent kinase 5 (Tyr15) (CDK5, 1:2000, Sigma), rabbit-anti-CDK5 (1:2000, Abcam), rabbit-anti-caspase3 (1:2000, CST), rabbit-anti-divalent mental transporter 1 (DMT1, 1:1000, Alpha diagnostic), rabbit-anti-p-extracellular regulated protein kinases1/2 (Thr202/Thr204) (ERK1/2, 1:2000, CST), rabbit-anti-ERK1/2 (1:2000, CST), goat-anti-ferroportin 1 (Fpn 1, 1:1000, Santa Cruz), rabbit-anti-glial fibrillary acidic protein (GFAP, 1:1000, Sigma), rabbit-anti-glutathione peroxidase 4 (GPx4, 1:1000, Santa Cruz), rabbit-anti-p-glycogen synthase kinase 3 alpha/βeta (Ser21/9) (p-GSK3α/β, 1:2000, CST), rabbit-anti-GSK3α/β (1:2000, CST), rabbit-anti-ionized binding adaptor protein 1 (Iba1, 1:1000, Abcam), rabbit-anti-interleukin 1 beta (IL-1β, 1:1000, Santa Cruz), mouse-anti-p-SAPK/JNK (Thr183/Tyr185) (1:2000, CST), rabbit-anti-SAPK/JNK (1:2000, CST), rabbit-anti-LC3A/B (1:2000, CST), rabbit-anti-NeuN (1:2000, CST), rabbit-anti-post-synaptic density protein 95 (PSD95, 1:2000, CST), rabbit-anti-p35/25 (1:2000, CST), rabbit-anti-protein phosphatase 2A C subunit (PP2A, 1:2000, CST), rabbit-anti-p-P38 mitogen-activated protein kinase (Thr180/Tyr182) (p-P38 MAPK, 1:2000, CST), rabbit-anti-P38 MAPK (1:2000, CST), rabbit-anti-superoxide dismutase 1 (SOD1, 1:1000, CST), mouse-anti-synaptophysin (SYP, 1:2000, Sigma), mouse-anti-tumor necrosis factor alpha (TNFα, 1:500, Santa Cruz), mouse-anti-transferrin receptor (TFR, 1:1000, Invitrogen), mouse-anti-Tau (Tau46) (1:2000, CST), rabbit-anti-p-Tau (Thr181) (1:2000, CST), rabbit-anti-p-Tau (Ser416) (1:2000, CST), rabbit-anti-p-Tau (Ser202) (1:2000, CST), rabbit-anti-p-Tau (Ser396) (1:1000, Sigma), rabbit-anti-p-Tau (Ser404) (1:2000, Sigma), rabbit-anti-p-Tau (Thr231) (1:1000, Sigma), rabbit-anti-cystine-glutamate antiporter (xCT, 1:2000, Abcam), and mouse-anti-β-actin (1:10000, Sigma). The membranes were then incubated with the respective horseradish peroxidase (HRP)-labeled secondary antibody after washing. Enhanced chemiluminescence (ECL) kits (Tanon, 250 ml) and Chem Doc XRS with Quantity One software (Bio-Rad, USA) were applied to detect blots. The quantification and analysis of band intensity were performed by ImageJ and GraphPad Prism 5.0 analysis software.

2.6. Immunohistochemistry

For evaluating morphological changes, brains from sacrificed mice were immediately fixed in 4% paraformaldehyde, then dehydrated and embedded in paraffin, and finally sliced into 5 μm sections. After dewaxing, the sections were sequentially treated with endogenous peroxidase blocking solution, L.A.B solution (Polyscience, Inc) and goat serum, and the sections were rinsed with Tris-buffered saline (TBS) three times after each treatment. Then, the sections were incubated with only one primary antibody overnight at 4 °C, and the primary antibodies used in immunohistochemistry were as follows: rabbit-anti-phospho-Tau (Ser416) (1:200, CST) and rabbit-anti-GFAP (1:200, Sigma). Next, the sections were treated with the corresponding biotinylated secondary antibody for 1 h at room temperature and then treated with a third antibody for 30 min. The sections were developed in DAB for 3 min, then immersed in distilled water to stop the reaction, and finally counterstained with hematoxylin. With these steps completed, the sections were dehydrated and sealed. The images of stained sections were collected on a light microscope (DM4000B; Leica).

2.7. Immunofluorescence

The antigens of frozen sections of brain tissue (10 μm and continuous) were repaired with L.A.B solution (Polyscience, Inc.) for 20 min. The sections were blocked with goat serum for 1 h and then incubated overnight at 4 °C with rabbit-anti-GPx4 (1:200, Santa Cruz). The sections were treated with a second fluorescence after washing and finally labeled by DAPI. The sections were then treated with MitoTracker Green (KGMP007, KeyGEN BioTECH) and incubated for 15 min at 37 °C, after washing four times the sections were sealed with antifade mounting medium. The sections were observed and photographed under the fluorescence microscope (Leica, SP8).

2.8. Improved iron staining

Due to the low iron content in mouse brain, the classic Prussian blue staining for assessing iron could not be used in this study [27]. An improved iron staining based on Prussian blue staining was applied. The paraffin sections (5 μm) were dewaxed and hydrated and then immersed in 0.1 M TBS (pH 7.4) containing 3% hydrogen peroxide (H_2O_2) for 10 min. After that, the sections were treated with an equal ratio mixture of 4% aqueous potassium ferrocyanide and 4% hydrochloric acid for 30 min. They were rinsed with ddH_2O for 5 min, and the iron staining was amplified with TBS containing 0.025% DAB and 0.0033% H_2O_2 for 10 min. This step was performed under a microscope to stop the reaction when brown granules were observed in the iron deposit regions. All the sections were handled in parallel to maintain consistency of the dyeing condition. Then, the sections were stained with hematoxylin, differentiated and sealed. Finally, the sections were observed and photographed under a microscope (DM4000B; Leica).

2.9. Calcium analysis

An Agilent inductively coupled plasma mass spectrometer 7500a (ICP-MS, Agilent Technologies Inc) was used to determinate the amount of calcium in the brain. Brain tissue samples of each mouse (n = 7) were accurately weighed prior to ICP-MS analysis, and the samples were then treated with 500 μl nitric acid (Sigma, Purity ≥ 90%) at 110 °C for 30 min. After returning to room temperature, the samples were diluted 20 times with distilled water, and the concentration of calcium in the diluent was quantified by ICP-MS.

2.10. Iron analysis

The brain and serum iron content was assayed as previously described using a flame atomic absorption spectrometer (ZEEnit700P, Analytikjena, Germany) [31].

2.11. Measurement of ROS and total SOD activity

To determine whether LA treatment decreased oxidative stress (free radical damage), ROS production was measured using 2′,7′-dichlorofluorescein diacetate (DCFH-DA) according to the manufacturer's protocol (E004, Jiancheng Biology, Nanjing, China). Briefly, cortices of mice brain were accurately weighed and homogenized in the ice-cold lysis buffer (10 mM Tris-HCl, 100 mM sucrose, 10 mM EDTA; pH 7.4; 1:20, w/v). The supernatant was collected by centrifugation at 1000 g for 10 min at 4 °C. The cell pellets were suspended with prechilled PBS. Cells at a density of 2×10^6/ml were incubated in 10 μM DCFH-DA at 37 °C for 60 min. The negation controls were incubated with PBS. The procedure was protected from light. DCF fluorescence intensity was measured at 485 nm excitation and 525 nm emission wavelengths using a microplate reader (Synergy/H1, BioTek). Total SOD activity was determined by the hydroxylamine method, and the brain samples were formed into homogenates in 0.9% normal saline (dilution method was 1 g : 9 ml) after weighting. Then, the homogenates were centrifuged at 2500–3000 r/min for 10 min, and the supernatants were used for detection. Detection was performed according to the manufacturer's instructions (A001-1, Jiancheng Biology, Nanjing, China).

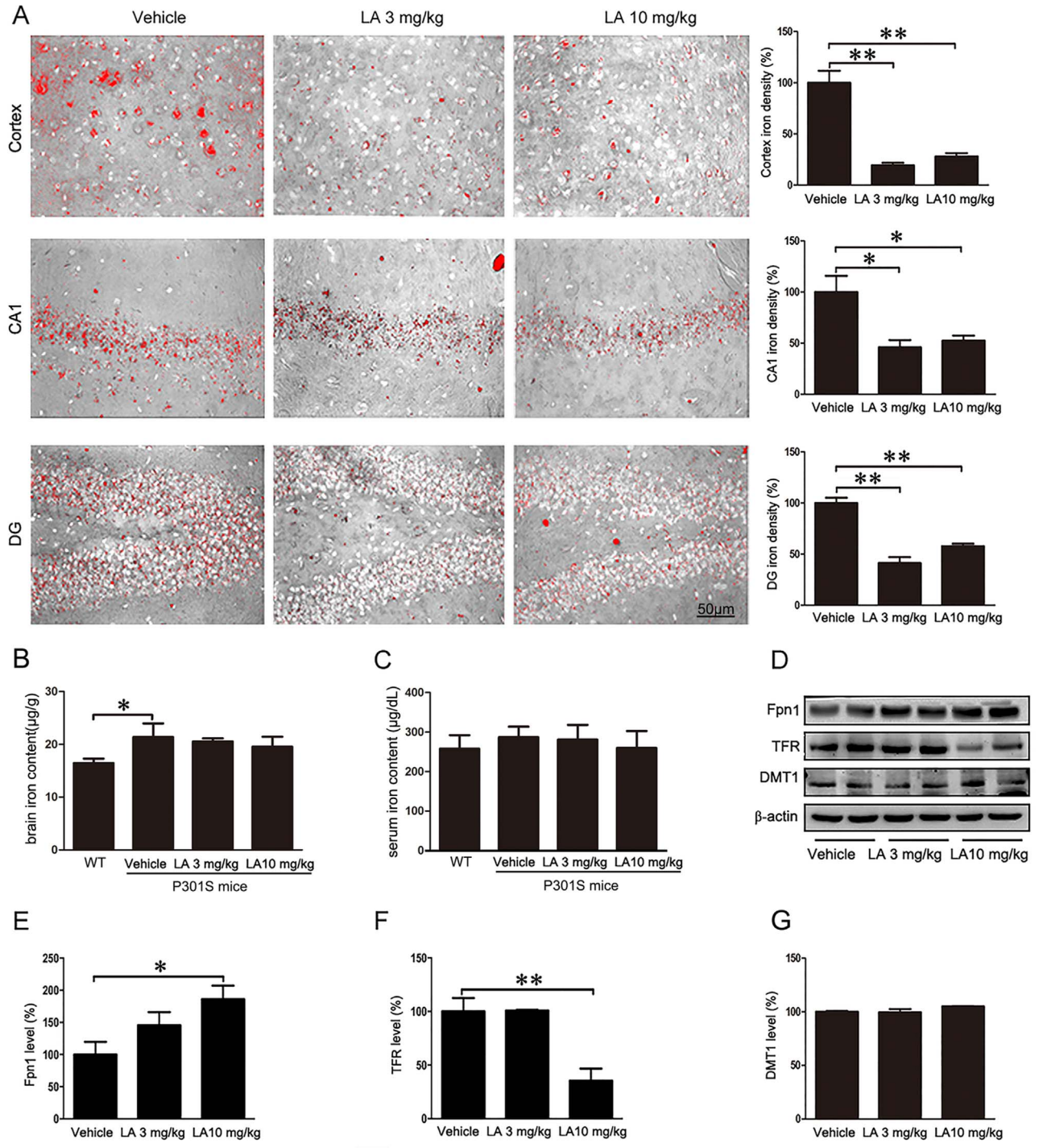

Fig. 1. LA mediated the distribution of iron in the brains of P301S mice. (A) Iron staining and the quantitative analysis of 9-month-old P301S mouse brains. The iron-staining results were processed by ImageJ to allow iron deposits to be easily observed as red granules. **(B, C)** Detection of iron content in the brain and serum by atomic absorption spectrometry. **(D-G)** Western blot analysis and quantification of Fpn1, TFR, and DMT1 with β-actin as an internal control. All results are presented as the mean ± SEM (n = 7). *p < 0.05, **p < 0.01.

2.12. Statistical analysis

All results were obtained from three repeated experiments and presented as the mean ± SEM. We employed one-way ANOVA for comparisons of three groups. The analyses were performed using ImageJ software and GraphPad Prism 5.0 software. The results were considered to have significant differences when **p < 0.01 or *p < 0.05.

3. Results

3.1. Effect of LA on the distribution of iron in P301S mice

We first examined the effects of LA treatment on iron distribution in P301S mice brains, and improved iron staining and iron deposits (brown granules) were observed in the cytoplasm of iron-positive cells. To facilitate the observation of the results, we processed the iron-staining results with ImageJ software so that the iron deposits could be easily observed as red granules. We found more iron-positive cells in

the cortex and hippocampus of the vehicle-treated mice than in the LA-treated mice (Fig. 1A, $p < 0.05$). We further determined the iron content in the brains of wild-type (WT) mice, P301S Tg mice, low-dose LA-treated mice and high-dose LA-treated mice. As shown in Fig. 1B, atomic absorption spectrum analysis revealed that iron levels were statistically higher in the brains of P301S mice than in WT mice (Fig. 1B, $p < 0.05$), but LA administration did not significantly alter the iron content in the brains of P301S mice (Fig. 1B, $p > 0.05$). No significant difference of in serum iron content was observed among WT mice, P301S mice, low-dose LA-treated mice and high-dose LA-treated mice (Fig. 1C, $p > 0.05$).

To investigate the mechanisms involved in the altered iron distribution, we next examined the effects of LA on the expression of TFR, DMT1 and the only known iron release protein, Fpn1. The expression of TFR in high-dose LA-treated mice was found to be significantly lower than that in vehicle-treated groups (Fig. 1D, F, $p < 0.01$). Treatment with high-dose LA induced a significant enhancement in Fpn1 expression compared with Fpn1 expression in vehicle-treated mice (Fig. 1D, E, $p < 0.05$). In addition, no significant difference in DMT1 expression was observed (Fig. 1D, G, $p > 0.05$). These results revealed that the iron redistribution in P301S mouse brains by LA mediated the expression of TFR and Fpn1 but not DMT1.

3.2. LA inhibited inflammation in P301S mice

Given the essential role of inflammation in tauopathy [1], we next examined the levels of inflammatory markers and pro-inflammatory proteins in P301S mice. As shown in Fig. 2B, high-dose LA treatment markedly down-regulated the levels of GFAP, TNFα and IL-1β compared to the levels in vehicle-treated mice (Fig. 2B, C-F, $p < 0.05$). GFAP immunoreactivity also exhibited a significant decrease in the cortex and hippocampus of high-dose LA-treated mice (Fig. 2A, $p < 0.05$). However, LA treatment did not significantly decrease the level of Iba1 (Fig. 2B, D, $p > 0.05$).

3.3. Effects of LA on oxidative stress

Oxidative stress is one of the key elements in the hyperphosphorylation and aggregation of Tau [12], we therefore determined the ROS levels in brain tissue, and the results showed that the level of ROS in high-dose LA-treated mice was significantly lower than that in vehicle-treated mice (Fig. 3A, $p < 0.05$). Western blot analyses demonstrated that the expression levels of GPx4, xCT and SOD1, which are important antioxidant enzymes in the oxidative stress balance, were highly upregulated after high-dose LA treatment compared with the levels in the vehicle-treated group (Fig. 3C-F, $p < 0.01$). In addition, the activity of SOD was also examined, and the results revealed a significant enhancement in high-dose LA-treated mice compared to that in vehicle-treated mice (Fig. 3B, $p < 0.05$). Immunofluorescence results using co-immunolabeling of GPx4 and MitoTracker Green indicated that GPx4 in the brains of LA-treated mice was more intense than that in vehicle-treated mice (Fig. 3H, $p < 0.05$). In addition, compared with that in vehicle-treated mice, the staining intensity of MitoTracker Green was significantly increased in the brains of LA-treated mice (Fig. 3H, $p < 0.05$). Finally, we determined calcium content in the brains of vehicle, low-dose and high-dose LA-treated mice, as shown in Fig. 3G, and ICP-MS analysis revealed that calcium levels were significantly lower in the brains of high-dose LA-treated mice than in the brains of vehicle-treated mice (Fig. 3G, $p < 0.05$).

Taken together, the results indicated that LA effectively attenuated oxidative stress in P301S mouse brains.

3.4. LA reduced p-Tau at multiple AD-related sites in P301S mice

We also examined the effect of LA on the level of hyperphosphorylated Tau, which is a major pathological feature in AD. Immunohistochemistry of phospho-Tau (Ser416) showed that the intensity of staining in the neurons of both the hippocampus and the cortex in the high-dose LA-treated mice was significantly lower than that in vehicle-treated mice (Fig. 4A, $p < 0.05$). As shown in Fig. 4B, treatment with high-dose LA resulted in a remarkable reduction in Tau phosphorylation at the Ser-202, Ser-396, Ser-404, Ser-416, and Thr-181 residues compared with the vehicle-treated group (Fig. 4B, C-G, $p < 0.05$), whereas no significant difference in Thr-231 was observed among the three groups (Fig. 4B, H, $p > 0.05$). No significant change in total Tau (T-Tau) level was observed (Fig. 4B, I, $p > 0.05$). The low-dose LA did not cause significant reductions in these Tau residues compared to the vehicle-treated group, but it still played a role in inhibiting Tau phosphorylation, and these results indicated that LA might inhibit Tau hyperphosphorylation in a dose-dependent manner.

3.5. LA inhibited hyperphosphorylation of Tau through multiple pathways

Because MAPK, GSK3β, CDK5 pathways and PP2A are related to Tau phosphorylation [32,33], we examined the effects of LA treatment on the levels of these kinases and phosphatase. Quantification of the Western blot showed that the high-dose LA treatment significantly decreased the level of p-P38 (Fig. 5A, D, $p < 0.05$) without affecting the phosphorylation of ERK1/2 and JNK1/2 compared with the vehicle-treated group (Fig. 5A-C, $p > 0.05$). No significant changes in the levels of the total amount of the three proteins in brain tissues among the three groups were observed. As shown in Fig. 5E, there was a marked reduction in the levels of calpain1 and in the ratios of p-CDK5/CDK5 and P25/P35 in the mice following the high-dose LA treatment compared with the vehicle-treated group (Fig. 5E-H, $p < 0.05$). In addition, as presented in Fig. 5I, the p-GSK3β (Ser9)/GSK3β ratio in the brains of high-dose LA-treated mice was significantly higher than that in the vehicle-treated group (Fig. 5I, K, $p < 0.05$), but there was no significant difference in the ratio of p-GSK3α/GSK3α (Fig. 5I, J, $p > 0.05$). We further determined the level of PP2A, considering its effect in the dephosphorylation of Tau [34]. As shown in Fig. 5I, the high-dose LA treatment induced a notable enhancement in PP2A expression compared with the vehicle-treated group (Fig. 5I, L, $p < 0.05$). These results indicated that PP2A plays a part in inhibiting the phosphorylation of Tau.

3.6. LA attenuated synaptic loss and apoptosis

Next, we examined the effect of LA on the alterations of synapses because Tau and p-Tau oligomers are widely perceived as contributing to synaptic dysfunction and loss [35]. As shown in Fig. 6A, the expression levels of SYP and PSD95, which are markers of pre- and postsynaptic compartments, were detected by Western blot. The results showed that the expression of SYP was significantly higher in the high-dose LA-treated group compared with the vehicle-treated group (Fig. 6A, C, $p < 0.05$), but no significant difference in PSD95 level was observed (Fig. 6A, D, $p > 0.05$).

Accumulation of p-Tau may cause apoptosis and affect the flux of autophagy, eventually leading to neurodegeneration [36,37]. To determine whether LA affected neurodegeneration in P301S mice, NeuN was examined using Western blot. Compared with the vehicle-treated mice, the high-dose LA-treated mice showed significantly increased NeuN levels (Fig. 6A, B, $p < 0.05$). To determine the related mechanisms, we examined the expression of AIF, Bcl2, Bax, and caspase3, which are involved in apoptosis. As shown in Fig. 6E, the ratio of cleaved caspase3/caspase3 was significantly lower in the high-dose LA-treated mice than in the vehicle-treated mice (Fig. 6E, H, $p < 0.01$). However, there were no significant differences in the levels of AIF and Bcl2/Bax among the three groups (Fig. 6E-G, $p > 0.05$), suggesting that LA inhibited apoptosis might mainly through a caspase-dependent pathway. The autophagy marker protein LC3A/B and Beclin1 were also detected utilized Western blot. No differences were detected in the

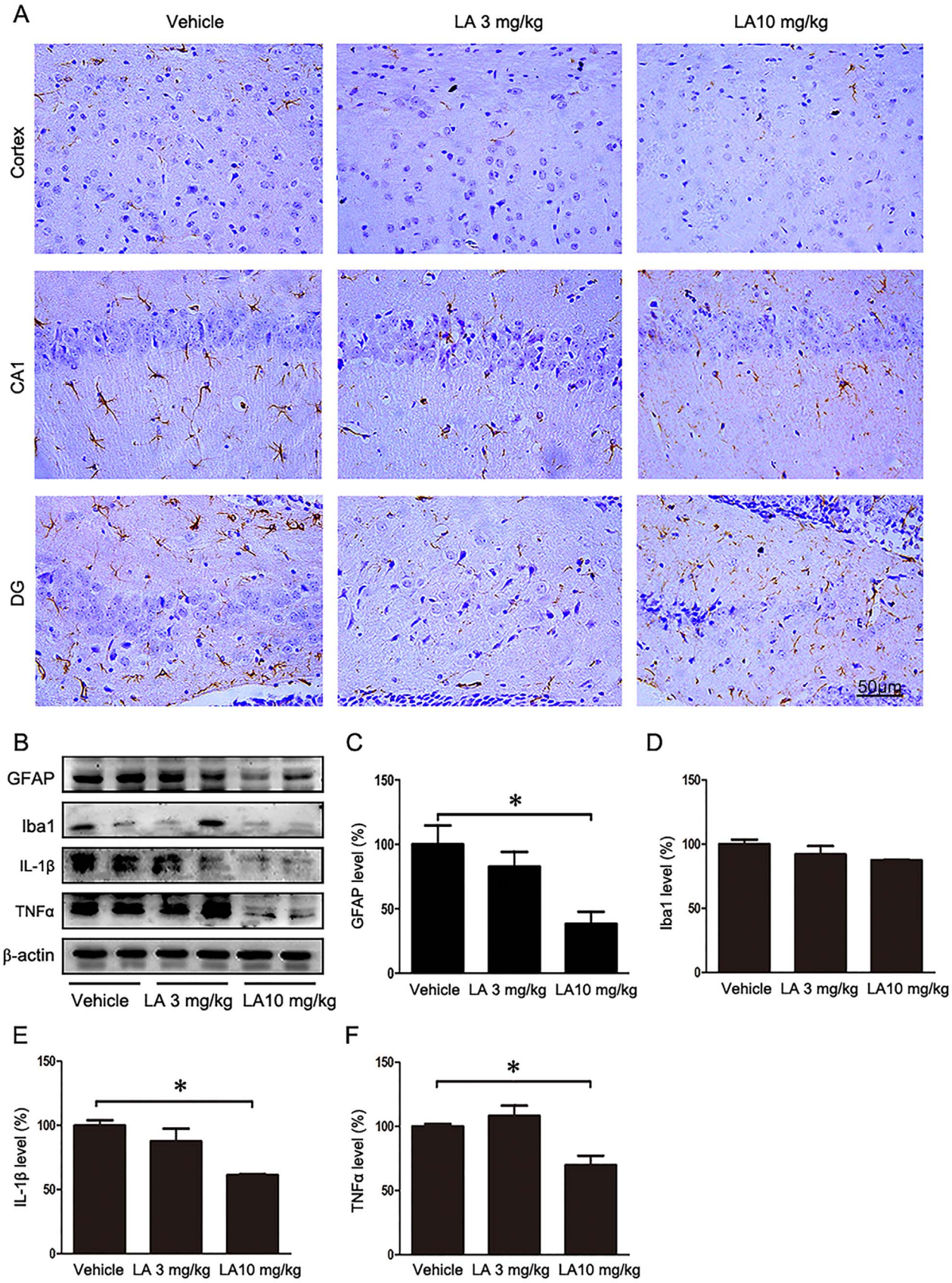

Fig. 2. Effect of LA on neuroinflammation in P301S mice. **(A)** GFAP-stained sections through the hippocampus or cortex in vehicle-, low-dose LA- and high-dose LA-treated mice. **(B)** Western blot analysis of GFAP, Iba1, IL-1β, and TNFα. **(C-F)** Quantitative analyses of Western blot for GFAP, Iba1, IL-1β and TNFα. β-actin was used as an internal control. All results are presented as the mean ± SEM (n = 7). *p < 0.05, **p < 0.01.

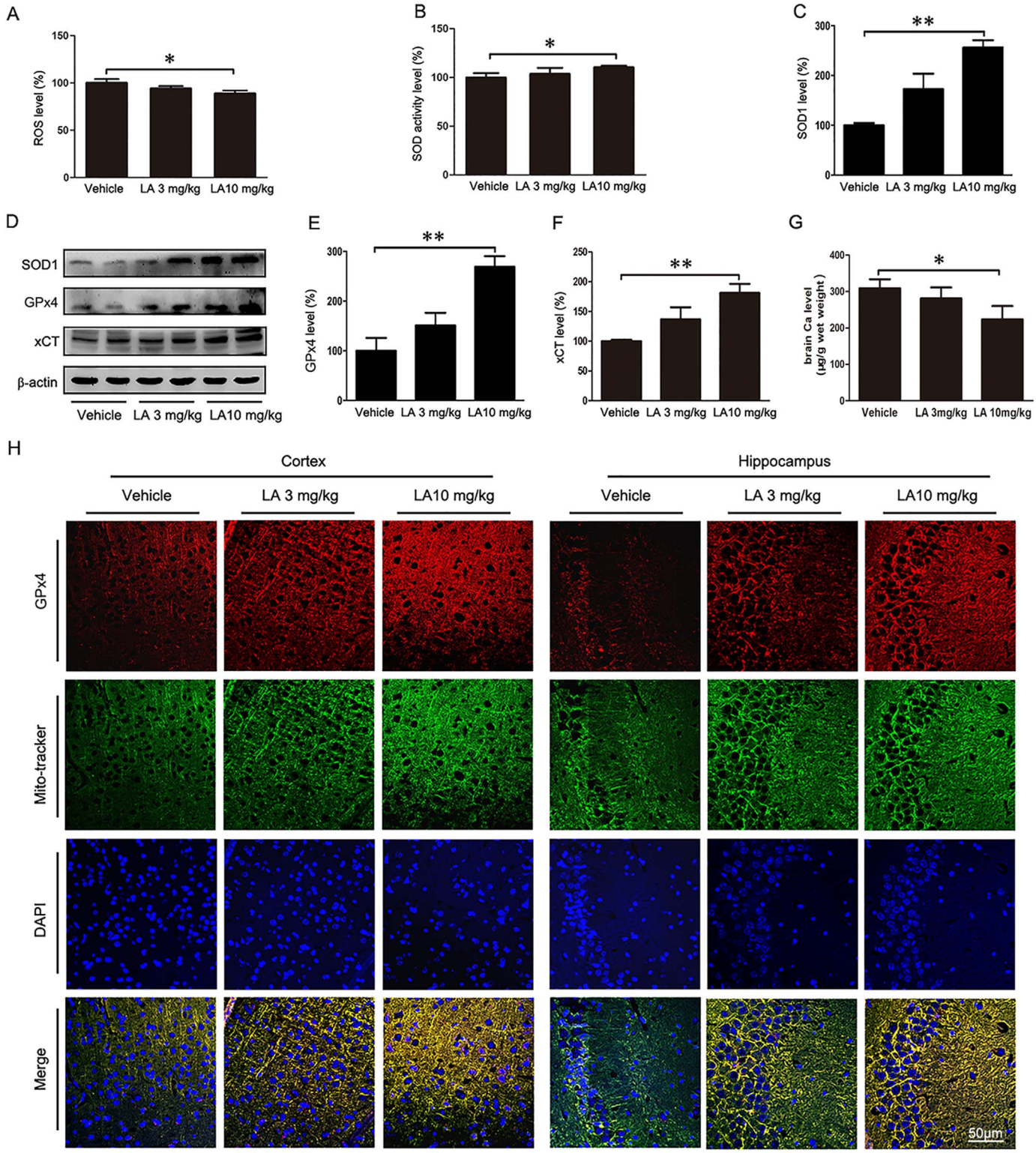

Fig. 3. Effect of LA on oxidative stress in the brains of P301S mice. (**A**) ROS production was detected in the brains of each group by the DCF-DA method. (**B**) SOD activity levels in the brains of each group. (**C-F**) Western blot and quantification analysis of SOD1, GPx4, and xCT with β-actin as a loading control. (**G**) Detection of calcium content by atomic absorption spectrometry. **(H)** Immunofluorescence with anti-GPx4 antibody and MitoTracker Green in the hippocampus and cortex. All results are presented as the mean ± SEM (n = 7). *$p < 0.05$, **$p < 0.01$.

LC3B/LC3A ratio and Beclin1 level among the three groups (Fig. 6E, I, J, $p > 0.05$). However, a dose-dependent activated trend in autophagy was observed, and whether a higher dose of LA could effectively active autophagy requires further study.

3.7. Effect of LA on learning ability and spatial memory in P301S mice

P301S mice are characterized by the main features of tau pathology leading to behavioral and cognitive disability at this early age [38,39]. To evaluate whether LA administration can ameliorate memory and

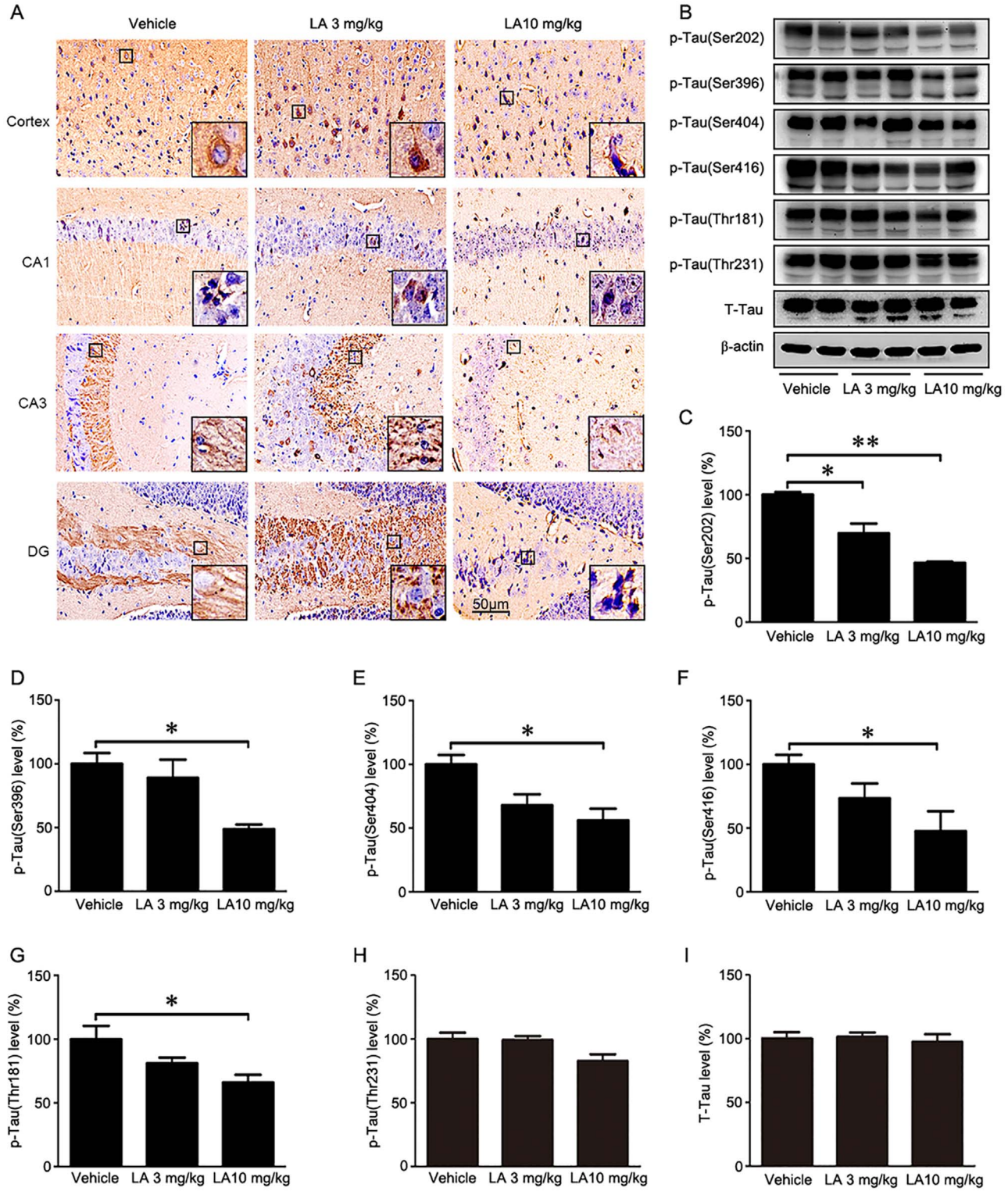

Fig. 4. LA inhibited Tau phosphorylation at multiple AD-related sites. (A) Detection of Tau phosphorylation in the brain by immunohistochemistry using anti-phospho-Tau (Ser416). **(B)** Western blot analysis of phosphorylated Tau at residues Ser-202, Ser396, Ser404, Ser-416, Thr181, and Thr231 in the brain. β-actin served as a loading control. **(C-I)** Quantitative analysis of Tau phosphorylation levels at Ser-202, Ser396, Ser404, Ser-416, Thr181, and Thr231 sites. All results are presented as the mean ± SEM (n = 7). *p < 0.05, **p < 0.01.

cognitive damage in P301S mice, OFT, MWM and NOR were performed as described above. In OFT, we observed no noticeable changes in total distance following 5 min of open field exploration among the three groups, indicating that locomotion was not affected by LA (Fig. 7D, $p > 0.05$). However, we observed that high-dose LA treatment significantly increased the time traveled by mice in the center of the open field compared with the vehicle-treated mice (Fig. 7E, $p < 0.01$), suggesting a potential anti-anxiety effect of LA treatment.

Next, we employed the NOR test to evaluate the role of LA in memory formation. After three days of adaptation, mice were exposed to two identical objects for 10 min. Twenty-four hours later, one of the familiar objects was replaced by a novel object, and then a 10-min test was conducted during which animals could freely explore the familiar and novel objects. Location preference index (LI, a ratio of the time

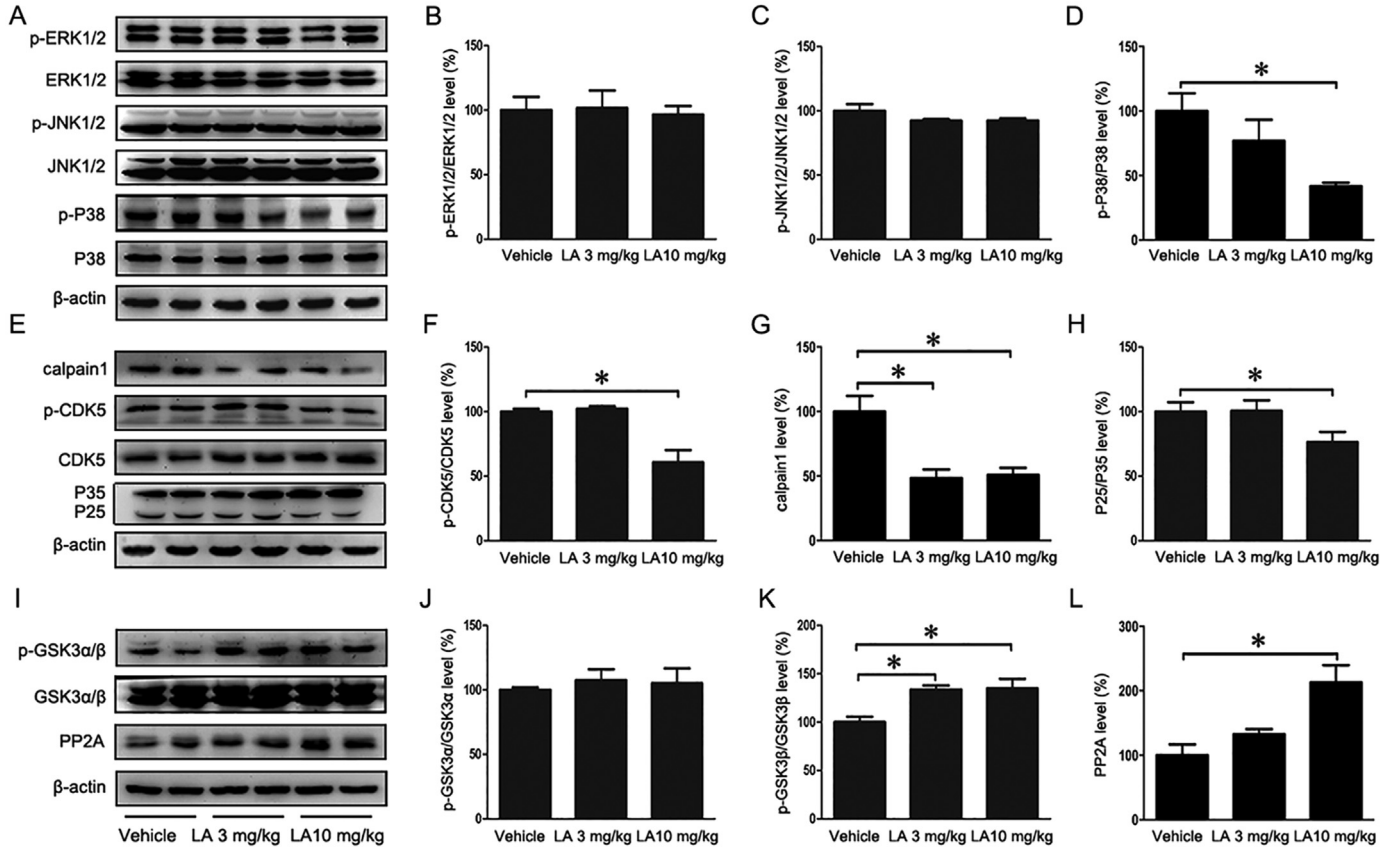

Fig. 5. LA inhibited P38 MAPK, calpain1/CDK5 and GSK3β pathways but promoted PP2A. (A) Western blotting analysis of p-ERK1/2, ERK1/2, p-JNK1/2, JNK1/2, p-P38, and P38. β-actin served as the loading control. (**B-D)** Quantitative analysis of p-ERK1/2, p-JNK1/2 and p-P38. (**E**) Western blot detection of calpain1, p-CDK5, CDK5 and P35/25 in the brains. (**F-H)** Quantification of calpain1, p-CDK5 and the P25/P35 ratio. **(I)** Western blot for p-GSK3α/β, GSK3α/β and PP2A expression. (**J-L)** Quantitative analysis of p-GSK3α, p-GSK3β and PP2A. All results are presented as the mean ± SEM (n = 7). *p < 0.05, **p < 0.01.

spent with the left/right object and the total time) and recognition index (RI, a ratio of time spent with the novel object and the total time) were used as measures to evaluate memory formation. We identified no differences in LI among the three groups, suggesting that there was no particular preference for the two positions (Fig. 7G, $p > 0.05$). However, the high-dose LA-treated group of mice demonstrated greater exploration of the novel object over the familiar object compared with the vehicle-treated mice (Fig. 7H, $p < 0.05$). The results revealed that high-dose LA-treated mice exhibited better memory.

To further assess the hippocampus-dependent spatial learning of mice, the MWM was employed. As shown in Fig. 7A, there were no differences in the latency among the three groups in the visible platform trial (Fig. 7A, $p > 0.05$), while the LA-treated mice exhibited significantly improved spatial learning compared with the vehicle-treated mice based on latency to reach the hidden platform (Fig. 7A, $p < 0.05$). Then, the spatial memory retention was assessed by a probe trial. The high-dose LA-treated mice showed significantly more platform location crossings than the vehicle-treated mice (Fig. 7B, $p < 0.01$). The results suggested that high-dose LA helps ameliorate spatial learning impairments. Fig. 7C shows the typical swim-paths in the hidden platform trial. The mouse with the mean escape duration nearest to the mean of the respective group was selected as an example swim-path LA-treated mice displayed better tendency to find the platform, and the spatial strategy of the mice was translated from a random pattern to a linear pattern. However, the swimming pattern of the vehicle-treated mice remained as a large loop.

Taken together, the results provide evidence of improved learning and spatial memory in LA-treated mice.

4. Discussion

Accumulating evidence has suggested the good prospects of Tau as a therapeutic target of AD. As a therapeutic agent in the treatment of DM, LA was reported to have neuroprotective functions against neurodegenerative diseases in clinical trials and in vitro/vivo studies [15–21,23,25,26]. However, whether LA can act on tauopathy and the implicated mechanism remain unknown. In the present study, we demonstrated that chronic treatment with LA significantly inhibited Tau hyperphosphorylation and alleviated neuronal degeneration and memory deficits in P301S mice. Moreover, our data also suggest the possible use of LA in inhibiting ferroptosis.

P301S Tg mice, which carry the human Tau gene with the P301S mutation, have been used to develop Tau pathology and to study its effects on neurodegeneration [38,39]. This well characterized mouse model has also been used to investigate novel therapeutic strategies of tau-related disorders [40,41]. Here, we first verified that iron levels were statistically higher in the brains of P301S mice at the age of 9 months than in the brains of WT mice. Because prior studies have shown iron aggregates in neurons with NFTs during the course of AD development [42,43], we sought to reduce iron concentration in the brains of P301S mice. In the current study, we observed that LA supplementation for 10 weeks did not significantly alter the levels of iron in the serum or brain, whereas the intensity of positive iron staining was significantly weakened in the hippocampus and the cortex of LA-treated mice compared with vehicle-treated mice. In addition, we assayed the expression of various iron transporters, including TFR, DMT1, and Fpn1, in the brains of P301S Tau Tg mice and found that LA supplementation induced a significant reduction in TFR expression and elevated Fpn1 protein. These results suggest that LA may regulate

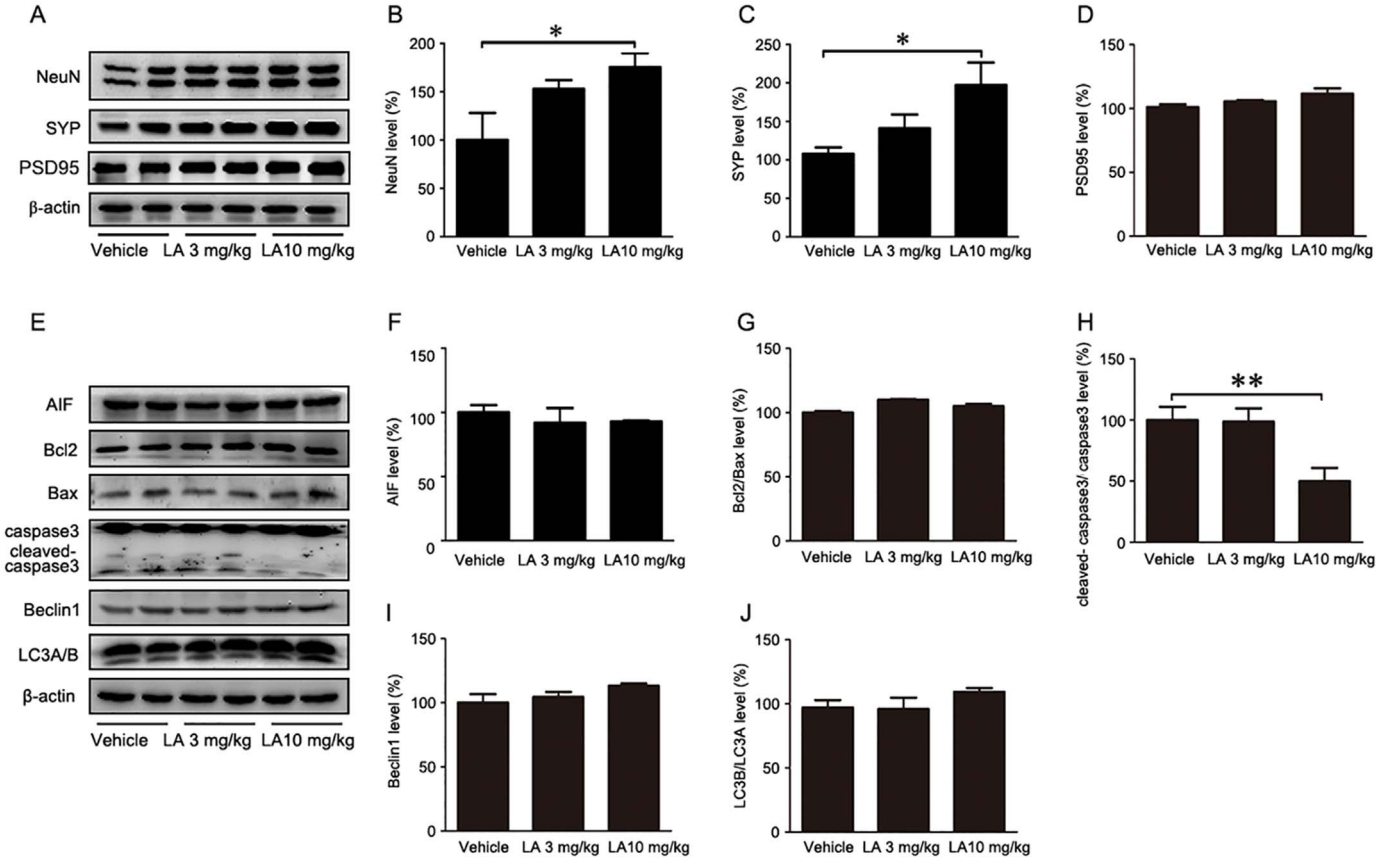

Fig. 6. LA rescued synaptic loss and inhibited apoptosis. (A-D) Western blot analysis and quantification of NeuN, SYP, and PSD95. β-actin is shown as a loading control. **(E)** Western blot analysis for AIF, Bcl2, Bax, caspase3, Beclin1, and LC3A/B. **(F-J)** Quantitative analysis of AIF, the Bcl2/Bax ratio, the cleaved caspase3/caspase3 ratio, Beclin1, and the LC3B/LC3A ratio. All results are presented as the mean ± SEM (n = 7). *p < 0.05, **p < 0.01.

intracellular iron concentration and mediate the redistribution of iron in specific areas of the mouse brain associated with neurodegeneration, namely, in the hippocampus, the neocortex, and in or around NFTs by LA-mediated chelation [11–14,44,45].

Of note, LA not only functions in the regulation of redistribution of iron via iron chelation but also reportedly acts as a direct free radical scavenger and an indirect antioxidant [14,24]. In support of this, we found that LA treatment was neuroprotective in P301S mouse brains by reducing ROS content, increasing SOD1 activity, and increasing the expression level of antioxidant enzymes (GPx4, xCT, and SOD1). Despite criticism and the limitations described in the literature, the DCFH method can be applicable for quick and basic screening experiments to provide a broad range of general ROS production [46]. These rescued antioxidant enzymes by LA effectively scavenged lipid peroxidation, suggesting that the protective effects of LA may be similar to our previously reported DFO-mediated chelation [47]. In addition, it has also been proposed that LA may play a protective role as an anti-inflammatory agent in AD [25]. In this regard, we also observed decreased expression of pro-inflammatory proteins, including IL-1β and TNF-α, which are released from activated microglia and astroglia.

A previous study identified that P301S mice sustained strong oxidative stress and eventually led to aggravated Tau hyperphosphorylation [48]. Furthermore, mounting evidence has been documented that iron can bind to Tau and contribute to its hyperphosphorylation, enhancing the toxicity of Tau to neurons [10–12]. To explain the antioxidant and anti-inflammatory roles as possible contributors that attenuate Tau pathology, Tau phosphorylation was examined in P301S mice with LA supplementation. Not surprisingly, the present data show that AD-related sites (Ser-202, Ser-396, Ser-404, Ser-416, Thr-181, and Thr-231) of Tau phosphorylation were remarkably inhibited by LA in a dose-dependent manner. Several studies have shown that Tau hyperphosphorylation occurs at more than 40 serine or threonine residues in AD [49–51], and dysregulation of multiple Tau kinases and Tau phosphatases might be responsible for most of the abnormal hyperphosphorylation of Tau in AD brains [52]. Thus, we further analyzed the mechanisms underlying the inhibitory effect of LA on Tau phosphorylation by examining the activities of several kinases, including CDK5, GSK3β, and MAPK, in P301S mouse brains. Consistent with the above mechanism, although we did not observe alterations in either ERK1/2 or JNK1/2 kinase activity at the tissue level, the activity of CDK5, GSK3β, and P38 MAPK was markedly inhibited by LA treatment. Furthermore, the phosphorylation level of calpain1 was significantly decreased in the brains of LA-treated mice compared to vehicle-treated mice. In addition, the expression level of phosphatases (PP2A) was significantly increased after LA treatment, which is known to inhibit hyperphosphorylation of Tau [53]. Interestingly, calpain1, a calcium-dependent cysteine protease, has been associated with tauopathy development and neurodegeneration via modulating the activity of CDK5, GSK3β, and ERK1/2 in AD [54]. Notably, recent studies have reported that calpain inhibition significantly decreased p-P38 levels and was accompanied by eliminating oxidative stress [55,56]. In our present study, we found that LA not only inhibited the activity of calpain1 but also significantly decreased the calcium content of brain tissue in LA-treated mice. Given that the levels of intracellular calcium were increased by iron overload [57], the mechanism through which LA overcomes Tau hyperphosphorylation might involve multiple factors, and in particular, inhibiting the hyperactivation of calpains.

It is reported that P301S mice show prominent neuronal loss in the hippocampal CA1 area in addition to accumulation of hyperphosphorylated Tau, and suppressing mutant Tau expression by

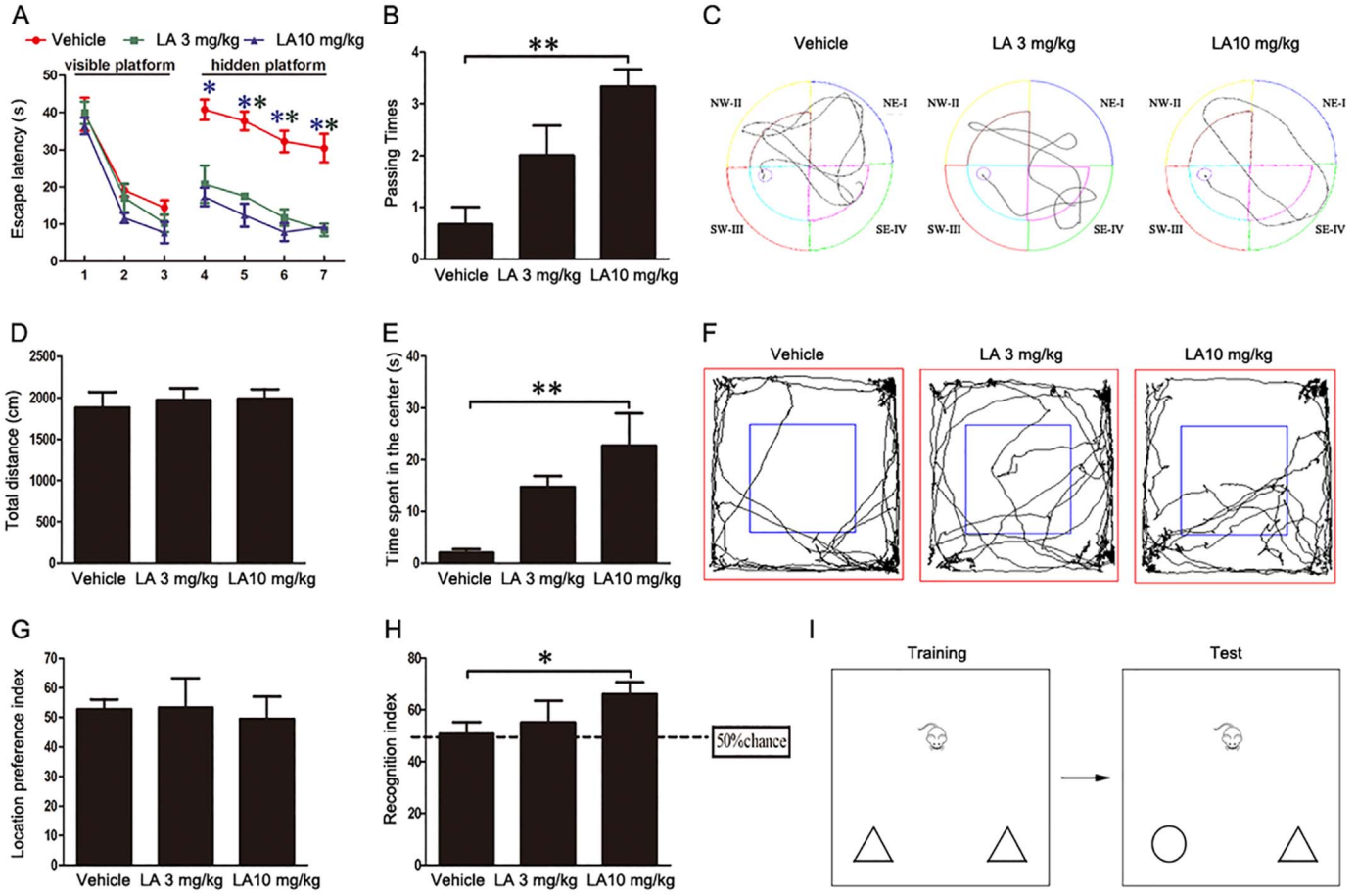

Fig. 7. LA-treated mice exhibited improved learning and spatial memory in behavioral tests. (A) Escape latency in the visible and hidden platform tests of the Morris water maze. **(B)** The passing times of the three groups in the probe trial of the Morris water maze test. **(C)** Graph of a typical path in the hidden platform trial of the Morris water maze test. **(D)** Total distance traveled during 5 min of open field exploration. **(E)** Time spent in the center of the open field during 5 min of open field exploration. **(F)** The movement tracks showing 5 min of open field exploration by the mice. **(G)** Location preference index was determined by the ratio of the time spent with the left object and the total time. **(H)** Recognition index was determined by the ratio of the time spent with the novel object and the total time. **(I)** Object placement in the training and test periods of the novel object recognition test. Two identical objects were presented in the training phase, and one of the familiar objects was replaced by a novel object in the test phase. All results are presented as the mean ± SEM (n = 7). *p < 0.05, **p < 0.01.

doxycycline treatment prevented further neuronal loss and improved memory function [39,58]. Because overactivated calpain can initiate and/or execute neuronal cell death along caspase-dependent and -independent pathways and increased levels of caspase-cleaved neurotoxic Tau form, calpain inhibition might confer additional neuroprotection in tauopathy by attenuating synaptic dysfunction and neurodegeneration. Thus, we further probed the cascade of events leading to apoptosis after LA supplementation. In the present study, we found that LA not only inhibited the high expression of calpain1 and cleaved caspase-3 but also improved the levels of NeuN and SYP, suggesting that the Tau-induced neuronal loss and synaptic dysfunction may be effectively inhibited by high-dose LA through the caspase-dependent pathway in P301S mice [59].

The greater iron content in the brain tissue of AD patients and animal models, together with the iron chelating action of LA, lead us speculate that the changed iron distribution presented in LA-treated mouse brains may be involved in the process of inhibiting neuronal ferroptosis, which is an iron-dependent type of cell death that is morphologically, biochemically and genetically distinct from apoptosis, various forms of necrosis, and autophagy [29]. Indeed, to date there is no clear mechanism of ferroptosis, but iron overload and the consequent lipid peroxidation and inflammation are considered as the three hallmarks of ferroptosis [60]. Importantly, ferroptosis may be a key mode of cell death in neurodegeneration [60,61]. Investigators have explored this possibility by testing the ability of iron chelators to prevent AD, and a number of iron chelators have been reported to have good potency in inhibiting neuronal loss [9,62,63]. Specifically, ferroptosis could be blocked by iron chelators deferoxamine (DFO) [64,65]. Therefore, it was worth considering whether neuronal populations important for cognition might be vulnerable to ferroptosis in the brains of P301S mice and whether LA can inhibit Tau-induced ferroptosis. As mentioned above, Fpn, the iron efflux pump, was increased, and TFR, the iron importer, was decreased in brain tissue of LA-treated mice. Therefore, intracellular iron overload in the cortex and the hippocampus might be reduced, and iron-dependent cell death might be depressed in the brains of LA-treated mice compared with vehicle-treated mice [64,66]. On the other hand, in agreement with the prevention of ferroptosis by lipophilic antioxidants [60,65,67], LA treatment can also inhibit the generation of ROS and increase the levels of GPx4 and xCT. During LA-treated neuronal loss, weakened neuroinflammatory factors may also have a central role in preventing Tau-induced ferroptosis. Aside from iron metabolism and lipid peroxidation signaling, activation of the MAPK pathway was thought to be involved in promoting ferroptosis [68,69]. In addition, a recently published study showed that active MAPK signaling can sensitize cells to ferroptosis via depleting cystine and reducing the expression of GPx4 [70]. In the present study, we found that LA blocked the activity of P38 in a dose-dependent manner, and GPx4 expression was significantly enhanced. Taken together, although we did not observe alterations in either morphology or genetics at the tissue level, we cannot eliminate

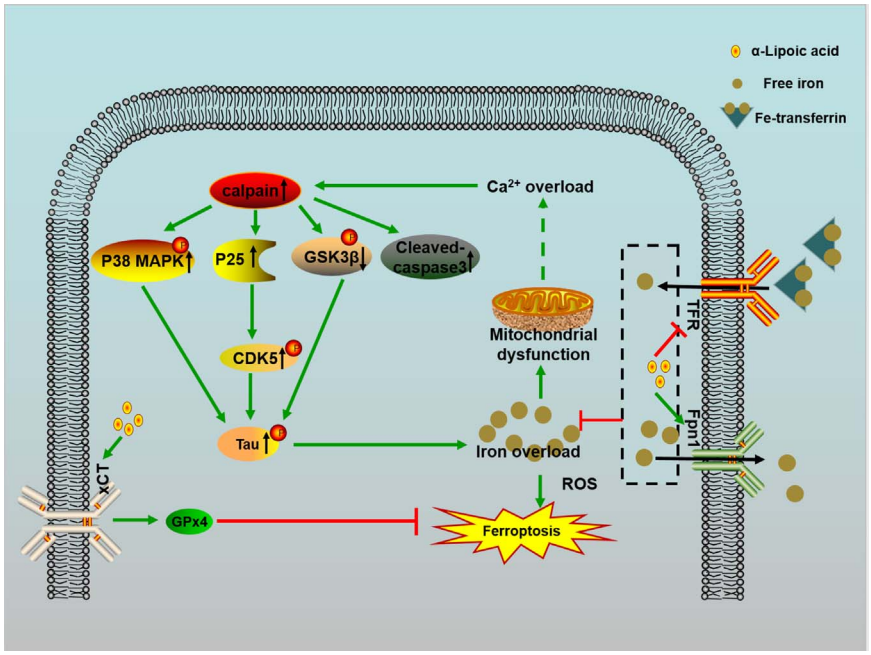

Fig. 8. Schematic diagram of the role of LA in inhibiting Tau phosphorylation and neuronal loss including ferroptosis. Under Tau overexpression and hyperphosphorylated conditions, P301S mice developed iron overload. After LA administration, TFR expression level was downregulated while Fpn1 level was upregulated, thereby reducing the iron overload. Thus, iron overload-induced mitochondrial dysfunction and Ca^{2+} overload were not sufficient to induce calpain overactivation. p-P38, P25, and p-CDK5 levels were decreased and p-GSK3β level was increased, thereby inhibiting the hyperphosphorylation of Tau and Tau-induced iron overload. In addition, LA inhibited ferroptosis not only by reducing iron overload but also via the upregulation of xCT and GPx4. Moreover, the inhibition of calpain decreased the level of cleaved caspase3, which is involved in apoptosis, thus neuronal loss was rescued through the inhibition of apoptosis and ferroptosis.

the role of ferroptosis in tauopathies, particularly because LA treatment blocked Tau hyperphosphorylation and enhanced neuronal survival in the P301S mice.

In light of the role of LA in regulating the development of AD-related tauopathies, we also considered the learning ability of the LA-treated mice. We observed that LA significantly improved the spatial memory and cognition capacity of the mice as measured by the MWM and the NOR and revealed by the obviously rescued locomotor and anxiety symptoms of the LA-treated mice in the OFT. Similar observations have been reported in old rats [18], in mouse models of AD [19–21], and in patients [15,16]. The improvements in cognitive and behavioral performances by LA observed here are in agreement with previous reports [25] and suggest that LA might play a role in regulating the development of tauopathy.

In summary, extensive experimental evidence, including our present findings, suggest that LA plays a neuroprotective role via its antioxidant and anti-inflammatory activity [15–21,23]. However, our data are the first to demonstrate that LA markedly protected neurons against Tau-induced neurotoxicity and cognitive impairment in P301S mice. A schematic diagram of the role of LA in inhibiting Tau phosphorylation and neuronal loss including ferroptosis is shown in Fig. 8. The schematic highlights that the cognitive impairments of P301S mice were relieved through several pathways, suggesting that LA may be used in potential treatment strategies for tauopathies and ultimately AD.

Acknowledgements

This study was financially supported by the Natural Science Foundation of China (U1608282), the Natural Science Foundation of Liaoning Province (No. 201602249).

Author contributions

Yan-Hui Zhang, performed most of the experiments and analyzed the data; Da-Wei Wang and Shuang-Feng Xu, contributed to experiments; Ying-Ying Yang, Shi-Qi Guo, Shan Wang, and Tian Guo, generated and validated the mouse model; Shuai Zhang and Yong-Gang Fan contributed to discussion. Zhan-You Wang, reviewed and edited manuscript, Chuang Guo designed and wrote manuscript. All authors have read and approved the final manuscript.

Compliance with ethical standards

All treatments were performed in accordance with the National Institutes of Health guidelines, and the experimental procedures were approved by the Laboratory Animal Ethical Committee of Northeastern University.

Conflict of interest

The authors declare that no competing interests exist.

References

[1] Y. Yoshiyama, M. Higuchi, B. Zhang, S.M. Huang, N. Iwata, T.C. Saido, J. Maeda, T. Suhara, J.Q. Trojanowski, V.M. Lee, Synapse loss and microglial activation precede tangles in a P301S tauopathy mouse model, Neuron 53 (3) (2007) 337–351, http://dx.doi.org/10.1016/j.neuron.2007.01.010.

[2] V.M. Lee, M. Goedert, J.Q. Trojanowski, Neurodegenerative tauopathies, Annu. Rev. Neurosci. 24 (2001) 1121–1159, http://dx.doi.org/10.1146/annurev.neuro.24.1.1121.

[3] S.L. DeVos, R.L. Miller, K.M. Schoch, B.B. Holmes, C.S. Kebodeaux, A.J. Wegener, G. Chen, T. Shen, H. Tran, B. Nichols, T.A. Zanardi, H.B. Kordasiewicz, E.E. Swayze, C.F. Bennett, M.I. Diamond, T.M. Miller, Tau reduction prevents neuronal loss and reverses pathological tau deposition and seeding in mice with tauopathy, Sci. Transl. Med. 9 (374) (2017), http://dx.doi.org/10.1126/scitranslmed.aag0481.

[4] D.M. Holtzman, M.C. Carrillo, J.A. Hendrix, L.J. Bain, A.M. Catafau, L.M. Gault, M. Goedert, E. Mandelkow, E.M. Mandelkow, D.S. Miller, S. Ostrowitzki, M. Polydoro, S. Smith, M. Wittmann, M. Hutton, Tau: from research to clinical development. Alzheimer's & dementia, J. Alzheimer's Assoc. 12 (10) (2016) 1033–1039, http://dx.doi.org/10.1016/j.jalz.2016.03.018.

[5] M. Perez, R. Cuadros, M.A. Smith, G. Perry, J. Avila, Phosphorylated, but not native, tau protein assembles following reaction with the lipid peroxidation product, 4-hydroxy-2-nonenal, FEBS Lett. 486 (3) (2000) 270–274.

[6] A. Takeda, M.A. Smith, J. Avila, A. Nunomura, S.L. Siedlak, X.W. Zhu, G. Perry, L.M. Sayre, In Alzheimer's disease, heme oxygenase is coincident with Alz50, an epitope of tau induced by 4-hydroxy-2-nonenal modification, J. Neurochem. 75 (3) (2000) 1234–1241, http://dx.doi.org/10.1046/j.1471-4159.2000.0751234.x.

[7] L. Lyras, N.J. Cairns, A. Jenner, P. Jenner, B. Halliwell, An assessment of oxidative damage to proteins, lipids, and DNA in brain from patients with Alzheimer's disease, J. Neurochem. 68 (5) (1997) 2061–2069.

[8] D. Berg, M.B. Youdim, Role of iron in neurodegenerative disorders, Top. Magn. Reson. Imaging 17 (1) (2006) 5–17, http://dx.doi.org/10.1097/01.rmr.0000245461.90406.ad.

[9] R.J. Ward, F.A. Zucca, J.H. Duyn, R.R. Crichton, L. Zecca, The role of iron in brain ageing and neurodegenerative disorders, Lancet Neurol. 13 (10) (2014) 1045–1060, http://dx.doi.org/10.1016/S1474-4422(14)70117-6.

[10] J. Garcia de Ancos, I. Correas, J. Avila, Differences in microtubule binding and self-association abilities of bovine brain tau isoforms, J. Biol. Chem. 268 (11) (1993) 7976–7982.

[11] M.D. Ledesma, J. Avila, I. Correas, Isolation of a phosphorylated soluble tau fraction from Alzheimer's disease brain, Neurobiol. Aging 16 (4) (1995) 515–522.
[12] A. Yamamoto, R.W. Shin, K. Hasegawa, H. Naiki, H. Sato, F. Yoshimasu, T. Kitamoto, Iron (III) induces aggregation of hyperphosphorylated tau and its reduction to iron (II) reverses the aggregation: implications in the formation of neurofibrillary tangles of Alzheimer's disease, J. Neurochem. 82 (5) (2002) 1137–1147.
[13] L.M. Sayre, D.A. Zelasko, P.L.R. Harris, G. Perry, R.G. Salomon, M.A. Smith, 4-hydroxynonenal-derived advanced lipid peroxidation end products are increased in Alzheimer's disease, J. Neurochem. 68 (5) (1997) 2092–2097.
[14] H.L. Persson, Z. Yu, O. Tirosh, J.W. Eaton, U.T. Brunk, Prevention of oxidant-induced cell death by lysosomotropic iron chelators, Free Radic. Biol. Med. 34 (10) (2003) 1295–1305.
[15] K. Hager, M. Kenklies, J. McAfoose, J. Engel, G. Munch, Alpha-lipoic acid as a new treatment option for Alzheimer's disease – a 48 months follow-up analysis, J. Neural Transm. Suppl. 72 (2007) 189–193.
[16] K. Hager, A. Marahrens, M. Kenklies, P. Riederer, G. Munch, Alpha-lipoic acid as a new treatment option for Alzheimer [corrected] type dementia, Arch. Gerontol. Geriatr. 32 (3) (2001) 275–282.
[17] S.A. Farr, H.F. Poon, D. Dogrukol-Ak, J. Drake, W.A. Banks, E. Eyerman, D.A. Butterfield, J.E. Morley, The antioxidants alpha-lipoic acid and N-acetylcysteine reverse memory impairment and brain oxidative stress in aged SAMP8 mice, J. Neurochem. 84 (5) (2003) 1173–1183.
[18] J. Liu, E. Head, A.M. Gharib, W. Yuan, R.T. Ingersoll, T.M. Hagen, C.W. Cotman, B.N. Ames, Memory loss in old rats is associated with brain mitochondrial decay and RNA/DNA oxidation: partial reversal by feeding acetyl-L-carnitine and/or R-alpha -lipoic acid, Proc. Natl. Acad. Sci. USA 99 (4) (2002) 2356–2361, http://dx.doi.org/10.1073/pnas.261709299.
19] J.F. Quinn, J.R. Bussiere, R.S. Hammond, T.J. Montine, E. Henson, R.E. Jones, R.W. Stackman Jr., Chronic dietary alpha-lipoic acid reduces deficits in hippocampal memory of aged Tg2576 mice, Neurobiol. Aging 28 (2) (2007) 213–225, http://dx.doi.org/10.1016/j.neurobiolaging.2005.12.014.
[20] H. Sancheti, G. Akopian, F. Yin, R.D. Brinton, J.P. Walsh, E. Cadenas, Age-dependent modulation of synaptic plasticity and insulin mimetic effect of lipoic acid on a mouse model of Alzheimer's disease, PloS One 8 (7) (2013) e69830, http://dx.doi.org/10.1371/journal.pone.0069830.
[21] H. Sancheti, K. Kanamori, I. Patil, R. Diaz Brinton, B.D. Ross, E. Cadenas, Reversal of metabolic deficits by lipoic acid in a triple transgenic mouse model of Alzheimer's disease: a 13C NMR study, J. Cereb. Blood Flow. Metab.: Off. J. Int. Soc. Cereb. Blood Flow. Metab. 34 (2) (2014) 288–296, http://dx.doi.org/10.1038/jcbfm.2013.196.
[22] M.A. Lovell, C. Xie, S. Xiong, W.R. Markesbery, Protection against amyloid beta peptide and iron/hydrogen peroxide toxicity by alpha lipoic acid, J. Alzheimer's Dis. 5 (3) (2003) 229–239.
[23] K. Ono, M. Hirohata, M. Yamada, Alpha-lipoic acid exhibits anti-amyloidogenicity for beta-amyloid fibrils in vitro, Biochem. Biophys. Res. Commun. 341 (4) (2006) 1046–1052, http://dx.doi.org/10.1016/j.bbrc.2006.01.063.
[24] L. Rochette, S. Ghibu, C. Richard, M. Zeller, Y. Cottin, C. Vergely, Direct and indirect antioxidant properties of alpha-lipoic acid and therapeutic potential, Mol. Nutr. Food Res. 57 (1) (2013) 114–125, http://dx.doi.org/10.1002/mnfr.201200608.
[25] A. Maczurek, K. Hager, M. Kenklies, M. Sharman, R. Martins, J. Engel, D.A. Carlson, G. Munch, Lipoic acid as an anti-inflammatory and neuroprotective treatment for Alzheimer's disease, Adv. Drug Deliv. Rev. 60 (13–14) (2008) 1463–1470, http://dx.doi.org/10.1016/j.addr.2008.04.015.
[26] P.I. Moreira, P.L. Harris, X. Zhu, M.S. Santos, C.R. Oliveira, M.A. Smith, G. Perry, Lipoic acid and N-acetyl cysteine decrease mitochondrial-related oxidative stress in Alzheimer disease patient fibroblasts, J. Alzheimer's Dis. 12 (2) (2007) 195–206.
[27] C. Guo, P. Wang, M.L. Zhong, T. Wang, X.S. Huang, J.Y. Li, Z.Y. Wang, Deferoxamine inhibits iron induced hippocampal tau phosphorylation in the Alzheimer transgenic mouse brain, Neurochem. Int. 62 (2) (2013) 165–172, http://dx.doi.org/10.1016/j.neuint.2012.12.005.
[28] Y. Xie, W. Hou, X. Song, Y. Yu, J. Huang, X. Sun, R. Kang, D. Tang, Ferroptosis: process and function, Cell Death Differ. 23 (3) (2016) 369–379, http://dx.doi.org/10.1038/cdd.2015.158.
29] S.J. Dixon, K.M. Lemberg, M.R. Lamprecht, R. Skouta, E.M. Zaitsev, C.E. Gleason, D.N. Patel, A.J. Bauer, A.M. Cantley, W.S. Yang, B. Morrison 3rd, B.R. Stockwell, Ferroptosis: an iron-dependent form of nonapoptotic cell death, Cell 149 (5) (2012) 1060–1072, http://dx.doi.org/10.1016/j.cell.2012.03.042.
[30] S.J. Dixon, B.R. Stockwell, The role of iron and reactive oxygen species in cell death, Nat. Chem. Biol. 10 (1) (2014) 9–17, http://dx.doi.org/10.1038/nchembio.1416.
[31] S. Zhang, R. Chai, Y.Y. Yang, S.Q. Guo, S. Wang, T. Guo, S.F. Xu, Y.H. Zhang, Z.Y. Wang, C. Guo, Chronic diabetic states worsen Alzheimer neuropathology and cognitive deficits accompanying disruption of calcium signaling in leptin-deficient APP/PS1 mice, Oncotarget 8 (27) (2017) 43617–43634, http://dx.doi.org/10.18632/oncotarget.17116.
[32] W. Noble, V. Olm, K. Takata, E., O.M. Casey, J. Meyerson, K. Gaynor, J. LaFrancois, L.L. Wang, T. Kondo, P. Davies, M. Burns, V.R. Nixon, D. Dickson, Y. Matsuoka, M. Ahlijanian, L.F. Lau, K. Duff, Cdk5 is a key factor in tau aggregation and tangle formation in vivo, Neuron 38 (4) (2003) 555–565, http://dx.doi.org/10.1016/S0896-6273(03)00259-9.
[33] E. Rockenstein, M. Torrance, A. Adame, M. Mante, P. Bar-on, J.B. Rose, L. Crews, E. Masliah, Neuroprotective effects of regulators of the glycogen synthase kinase-3beta signaling pathway in a transgenic model of Alzheimer's disease are associated with reduced amyloid precursor protein phosphorylation, J. Neurosci. 27 (8) (2007) 1981–1991, http://dx.doi.org/10.1523/JNEUROSCI.4321-06.2007.
[34] F. Liu, I. Grundke-Iqbal, K. Iqbal, C.X. Gong, Contributions of protein phosphatases PP1, PP2A, PP2B and PP5 to the regulation of tau phosphorylation, Eur. J. Neurosci. 22 (8) (2005) 1942–1950, http://dx.doi.org/10.1111/j.1460-9568.2005.04391.x.
[35] K.J. Kopeikina, M. Polydoro, H.C. Tai, E. Yaeger, G.A. Carlson, R. Pitstick, B.T. Hyman, T.L. Spires-Jones, Synaptic alterations in the rTg4510 mouse model of tauopathy, J. Comp. Neurol. 521 (6) (2013) 1334–1353, http://dx.doi.org/10.1002/cne.23234.
[36] C. Ballatore, V.M.Y. Lee, J.Q. Trojanowski, Tau-mediated neurodegeneration in Alzheimer's disease and related disorders, Nat. Rev. Neurosci. 8 (9) (2007) 663–672, http://dx.doi.org/10.1038/nrn2194.
[37] T. Gomez-Isla, R. Hollister, H. West, S. Mui, J.H. Growdon, R.C. Petersen, J.E. Parisi, B.T. Hyman, Neuronal loss correlates with but exceeds neurofibrillary tangles in Alzheimer's disease, Ann. Neurol. 41 (1) (1997) 17–24, http://dx.doi.org/10.1002/ana.410410106.
[38] H. Xu, T.W. Rosler, T. Carlsson, A. de Andrade, J. Bruch, M. Hollerhage, W.H. Oertel, G.U. Hoglinger, Memory deficits correlate with tau and spine pathology in P301S MAPT transgenic mice, Neuropathol. Appl. Neurobiol. 40 (7) (2014) 833–843, http://dx.doi.org/10.1111/nan.12160.
[39] K. Santacruz, J. Lewis, T. Spires, J. Paulson, L. Kotilinek, M. Ingelsson, A. Guimaraes, M. DeTure, M. Ramsden, E. McGowan, C. Forster, M. Yue, J. Orne, C. Janus, A. Mariash, M. Kuskowski, B. Hyman, M. Hutton, K.H. Ashe, Tau suppression in a neurodegenerative mouse model improves memory function, Science 309 (5733) (2005) 476–481, http://dx.doi.org/10.1126/science.1113694.
[40] T. Jiang, Y.D. Zhang, Q. Chen, Q. Gao, X.C. Zhu, J.S. Zhou, J.Q. Shi, H. Lu, L. Tan, J.T. Yu, TREM2 modifies microglial phenotype and provides neuroprotection in P301S tau transgenic mice, Neuropharmacology 105 (2016) 196–206, http://dx.doi.org/10.1016/j.neuropharm.2016.01.028.
[41] Z. Ahmed, J. Cooper, T.K. Murray, K. Garn, E. McNaughton, H. Clarke, S. Parhizkar, M.A. Ward, A. Cavallini, S. Jackson, S. Bose, F. Clavaguera, M. Tolnay, I. Lavenir, M. Goedert, M.L. Hutton, M.J. O'Neill, A novel in vivo model of tau propagation with rapid and progressive neurofibrillary tangle pathology: the pattern of spread is determined by connectivity, not proximity, Acta Neuropathol. 127 (5) (2014) 667–683, http://dx.doi.org/10.1007/s00401-014-1254-6.
[42] P.F. Good, D.P. Perl, L.M. Bierer, J. Schmeidler, Selective accumulation of aluminum and iron in the neurofibrillary tangles of Alzheimer's disease: a laser microprobe (LAMMA) study, Ann. Neurol. 31 (3) (1992) 286–292, http://dx.doi.org/10.1002/ana.410310310.
[43] M.A. Smith, L.M. Sayre, V.M. Monnier, G. Perry, Oxidative posttranslational modifications in Alzheimer disease. A possible pathogenic role in the formation of senile plaques and neurofibrillary tangles, Mol. Chem. Neuropathol. 28 (1–3) (1996) 41–48, http://dx.doi.org/10.1007/BF02815203.
[44] A.C. Crespo, B. Silva, L. Marques, E. Marcelino, C. Maruta, S. Costa, A. Timoteo, A. Vilares, F.S. Couto, P. Faustino, A.P. Correia, A. Verdelho, G. Porto, M. Guerreiro, A. Herrero, C. Costa, A. de Mendonca, L. Costa, M. Martins, Genetic and biochemical markers in patients with Alzheimer's disease support a concerted systemic iron homeostasis dysregulation, Neurobiol. Aging 35 (4) (2014) 777–785, http://dx.doi.org/10.1016/j.neurobiolaging.2013.10.078.
[45] R.R. Crichton, D.T. Dexter, R.J. Ward, Brain iron metabolism and its perturbation in neurological diseases, J. Neural Transm. 118 (3) (2011) 301–314, http://dx.doi.org/10.1007/s00702-010-0470-z.
[46] A. Wojtala, M. Bonora, D. Malinska, P. Pinton, J. Duszynski, M.R. Wieckowski, Methods to monitor ROS production by fluorescence microscopy and fluorometry, Methods Enzymol. 542 (2014) 243–262, http://dx.doi.org/10.1016/B978-0-12-416618-9.00013-3.
[47] H. Xue, D. Chen, Y.K. Zhong, Z.D. Zhou, S.X. Fang, M.Y. Li, C. Guo, Deferoxamine ameliorates hepatosteatosis via several mechanisms in ob/ob mice, Ann. N. Y. Acad. Sci. 1375 (1) (2016) 52–65, http://dx.doi.org/10.1111/nyas.13174.
[48] M. Dumont, C. Stack, C. Elipenahli, S. Jainuddin, M. Gerges, N.N. Starkova, L. Yang, A.A. Starkov, F. Beal, Behavioral deficit, oxidative stress, and mitochondrial dysfunction precede tau pathology in P301S transgenic mice, FASEB J. 25 (11) (2011) 4063–4072, http://dx.doi.org/10.1096/fj.11-186650.
[49] J. Avila, The tau code, Front Aging Neurosci. 1 (2009), http://dx.doi.org/10.3389/neuro.24.001.2009.
[50] D.P. Hanger, B.H. Anderton, W. Noble, Tau phosphorylation: the therapeutic challenge for neurodegenerative disease, Trends Mol. Med. 15 (3) (2009) 112–119, http://dx.doi.org/10.1016/j.molmed.2009.01.003.
[51] J.Z. Wang, F. Liu, Microtubule-associated protein tau in development, degeneration and protection of neurons, Prog. Neurobiol. 85 (2) (2008) 148–175, http://dx.doi.org/10.1016/j.pneurobio.2008.03.002.
[52] K. Iqbal, F. Liu, C.X. Gong, C. Alonso Adel, I. Grundke-Iqbal, Mechanisms of tau-induced neurodegeneration, Acta Neuropathol. 118 (1) (2009) 53–69, http://dx.doi.org/10.1007/s00401-009-0486-3.
[53] C.X. Gong, T. Lidsky, J. Wegiel, L. Zuck, I. Grundke-Iqbal, K. Iqbal, Phosphorylation of microtubule-associated protein tau is regulated by protein phosphatase 2A in mammalian brain. Implications for neurofibrillary degeneration in Alzheimer's disease, J. Biol. Chem. 275 (8) (2000) 5535–5544.
[54] P.S. Vosler, C.S. Brennan, J. Chen, Calpain-mediated signaling mechanisms in neuronal injury and neurodegeneration, Mol. Neurobiol. 38 (1) (2008) 78–100, http://dx.doi.org/10.1007/s12035-008-8036-x.
[55] I.K. Aggeli, I. Beis, C. Gaitanaki, Oxidative stress and calpain inhibition induce alpha B-crystallin phosphorylation via p38-MAPK and calcium signalling pathways in H9c2 cells, Cell. Signal. 20 (7) (2008) 1292–1302, http://dx.doi.org/10.1016/j.cellsig.2008.02.019.
[56] K.H. Chang, Y. de Pablo, H.P. Lee, H.G. Lee, M.A. Smith, K. Shah, Cdk5 is a major regulator of p38 cascade: relevance to neurotoxicity in Alzheimer's disease, J. Neurochem. 113 (5) (2010) 1221–1229, http://dx.doi.org/10.1111/j.1471-4159.

2010.06687.x.
[57] D.G. Lee, J. Park, H.S. Lee, S.R. Lee, D.S. Lee, Iron overload-induced calcium signals modulate mitochondrial fragmentation in HT-22 hippocampal neuron cells, Toxicology 365 (2016) 17–24, http://dx.doi.org/10.1016/j.tox.2016.07.022.
[58] T.L. Spires, J.D. Orne, K. SantaCruz, R. Pitstick, G.A. Carlson, K.H. Ashe, B.T. Hyman, Region-specific dissociation of neuronal loss and neurofibrillary pathology in a mouse model of tauopathy, Am. J. Pathol. 168 (5) (2006) 1598–1607, http://dx.doi.org/10.2353/ajpath.2006.050840.
[59] B. Allen, E. Ingram, M. Takao, M.J. Smith, R. Jakes, K. Virdee, H. Yoshida, M. Holzer, M. Craxton, P.C. Emson, C. Atzori, A. Migheli, R.A. Crowther, B. Ghetti, M.G. Spillantini, M. Goedert, Abundant tau filaments and nonapoptotic neurodegeneration in transgenic mice expressing human P301S tau protein, J. Neurosci. 22 (21) (2002) 9340–9351.
[60] W.S. Hambright, R.S. Fonseca, L. Chen, R. Na, Q. Ran, Ablation of ferroptosis regulator glutathione peroxidase 4 in forebrain neurons promotes cognitive impairment and neurodegeneration, Redox Biol. 12 (2017) 8–17, http://dx.doi.org/10.1016/j.redox.2017.01.021.
[61] K. Ito, Y. Eguchi, Y. Imagawa, S. Akai, H. Mochizuki, Y. Tsujimoto, MPP + induces necrostatin-1- and ferrostatin-1-sensitive necrotic death of neuronal SH-SY5Y cells, Cell Death Discov. 3 (2017) 17013, http://dx.doi.org/10.1038/cddiscovery.2017.13.
[62] C.M. Cahill, D.K. Lahiri, X. Huang, J.T. Rogers, Amyloid precursor protein and alpha synuclein translation, implications for iron and inflammation in neurodegenerative diseases, Biochim. Biophys. Acta 1790 (7) (2009) 615–628, http://dx.doi.org/10.1016/j.bbagen.2008.12.001.
[63] S. Mandel, T. Amit, O. Bar-Am, M.B. Youdim, Iron dysregulation in Alzheimer's disease: multimodal brain permeable iron chelating drugs, possessing neuroprotective-neurorescue and amyloid precursor protein-processing regulatory activities as therapeutic agents, Prog. Neurobiol. 82 (6) (2007) 348–360, http://dx.doi.org/10.1016/j.pneurobio.2007.06.001.
[64] S. Ma, E.S. Henson, Y. Chen, S.B. Gibson, Ferroptosis is induced following siramesine and lapatinib treatment of breast cancer cells, Cell Death Dis. 7 (2016) e2307, http://dx.doi.org/10.1038/cddis.2016.208.
[65] R.E. Speer, S.S. Karuppagounder, M. Basso, S.F. Sleiman, A. Kumar, D. Brand, N. Smirnova, I. Gazaryan, S.J. Khim, R.R. Ratan, Hypoxia-inducible factor prolyl hydroxylases as targets for neuroprotection by "antioxidant" metal chelators: from ferroptosis to stroke, Free Radic. Biol. Med. 62 (2013) 26–36, http://dx.doi.org/10.1016/j.freeradbiomed.2013.01.026.
[66] D. Basuli, L. Tesfay, Z. Deng, B. Paul, Y. Yamamoto, G. Ning, W. Xian, F. McKeon, M. Lynch, C.P. Crum, P. Hegde, M. Brewer, X. Wang, L.D. Miller, N. Dyment, F.M. Torti, S.V. Torti, Iron addiction: a novel therapeutic target in ovarian cancer, Oncogene 36 (29) (2017) 4089–4099, http://dx.doi.org/10.1038/onc.2017.11.
[67] M.M. Gaschler, B.R. Stockwell, Lipid peroxidation in cell death, Biochem. Biophys. Res. Commun. 482 (3) (2017) 419–425, http://dx.doi.org/10.1016/j.bbrc.2016.10.086.
[68] N. Yagoda, M. von Rechenberg, E. Zaganjor, A.J. Bauer, W.S. Yang, D.J. Fridman, A.J. Wolpaw, I. Smukste, J.M. Peltier, J.J. Boniface, R. Smith, S.L. Lessnick, S. Sahasrabudhe, B.R. Stockwell, RAS-RAF-MEK-dependent oxidative cell death involving voltage-dependent anion channels, Nature 447 (7146) (2007) 864–868, http://dx.doi.org/10.1038/nature05859.
[69] Y. Yu, Y. Xie, L. Cao, L. Yang, M. Yang, M.T. Lotze, H.J. Zeh, R. Kang, D. Tang, The ferroptosis inducer erastin enhances sensitivity of acute myeloid leukemia cells to chemotherapeutic agents, Mol. Cell. Oncol. 2 (4) (2015) e1054549, http://dx.doi.org/10.1080/23723556.2015.1054549.
[70] I. Poursaitidis, X. Wang, T. Crighton, C. Labuschagne, D. Mason, S.L. Cramer, K. Triplett, R. Roy, O.E. Pardo, M.J. Seckl, S.W. Rowlinson, E. Stone, R.F. Lamb, Oncogene-selective sensitivity to synchronous cell death following modulation of the amino acid nutrient cystine, Cell Rep. 18 (11) (2017) 2547–2556, http://dx.doi.org/10.1016/j.celrep.2017.02.054.